


An improved upper-bound pushover procedure for seismic assessment of high-rise moment resisting steel frames

Abdallah Yacine Rahmani¹ · Nouredine Bourahla¹ · Rita Bento²  · Mohamed Badaoui³

Received: 16 December 2016 / Accepted: 18 July 2017 / Published online: 31 July 2017
© Springer Science+Business Media B.V. 2017

Abstract In recent years, nonlinear static procedures (NSPs) have gained considerable popularity as an efficient tool in the performance based seismic design practice. This was backed by extensive corroboration studies that have demonstrated its good accuracy in estimating the seismic response of regular structures. Despite the numerous improvements of the original versions of NSPs, their use to assess the seismic response of irregular structures and high-rise buildings is still challenging; they are not able to predict with sufficient accuracy all the complexities associated to the seismic response of this type of structures. Thus, an improved upper-bound (IUB) pushover procedure for seismic assessment of plane frames is presented in this paper, aiming to enhance the accuracy of existing methods in predicting the seismic behaviour of high-rise buildings. The novelty of this proposal is based on the adjustment of the pattern of the lateral load of the upper-bound pushover method applied to tall structures. The accuracy of the procedure is tested using nine, twelve, fifteen and twenty storeys steel buildings. The results of the (IUB) are compared to those of the capacity spectrum method, the modal pushover analysis, the upper bound pushover analysis, the modified upper bound pushover analysis and the non-linear time history analysis (NTHA). In most cases, the proposed procedure shows better results and closer to those obtained by NTHA.

Keywords Higher mode effects · Improved upper-bound pushover analysis · Steel buildings · Seismic loadings · Pushover analysis

✉ Rita Bento
rita.bento@tecnico.ulisboa.pt

¹ LGGC Laboratory, Department of Civil Engineering, Faculty of Technology, Blida 1 University, Blida, Algeria

² CERIS, Instituto Superior Técnico, Universidade de Lisboa, Lisbon, Portugal

³ LDMM Laboratory, Department of Civil Engineering, Faculty of Technology, Djelfa University, Djelfa, Algeria

1 Introduction

The trend in performance based seismic design (PBSD) practice has been a significant drive that led to a remarkable progress in simplified methods for seismic analysis based on the nonlinear static procedures (NSPs) in an attempt to obtain results close to those from nonlinear time history analysis (NTHA), which remains a sophisticated method at design and assessment level. The conventional NSPs or pushover analysis (Freeman 1998; Fajfar 1999), which considers the structural inelastic behaviour, is based on the assumption that the response of the structure is basically controlled by a single (fundamental) mode of vibration and the form of this mode remains constant throughout the duration of the seismic excitation. This assumption may be sometimes inadequate, particularly for buildings having a plan irregularity or high-rise buildings where higher modes may have an influence on the responses of such types of structures.

To overcome these limitations, while keeping the simplicity of the method, several researchers have proposed improvements on these procedures. Chopra and Goel (2002) have developed a modal pushover analysis (MPA) to include the contributions of all modes of vibration that have a significant influence on the seismic response. With a multi-run procedure and invariant lateral load, this method uses in each run a different distribution of lateral load proportional to each mode of vibration of the structure. The final results are obtained by combining the results calculated from each pushover curve using an appropriate combination rule (e.g. SRSS, CQC). The method has been extended to asymmetric-plan buildings (Chopra and Goel 2004) as well as bi-directional loadings (Reyes and Chopra 2011).

Paraskeva and Kappos (2010) proposed the improved modal pushover analysis (IMPA) that was successfully applied in the seismic assessment of bridges. IMPA is a multimode procedure that has the advantage of redefining the lateral load applied, considering the deformed shape of the structure when it is behaving nonlinearly. Still, in this procedure all modes are run independently and the interaction between them is neglected. Belejo and Bento (2016) explored the IMPA in asymmetric plan buildings; it has been concluded that there is only a slight improvement of the IMPA over the MPA which may not be enough to make of the IMPA a worthwhile method, since it doubles the calculation time consumption when compared to MPA.

Jan et al. (2004) on the other hand, proposed the Upper-Bound (UB) pushover analysis method to account for the effect of higher modes for two-dimensional (2D) tall building frames. The UB method proposes a new formula for determining the lateral load pattern and the upper-bound (absolute sum) modal combination rule for determining the target roof displacement. It has been shown that the use of modes higher than the second higher mode only give contribution ratios negligible for the prediction of the structural seismic response for tall buildings.

It was verified that UB method tends to significantly underestimate the seismic demands at the lower storeys of tall building frames. To overcome this limitation, Poursha and Samarin (2015) have modified the UB method, proposing the herein after called modified upper bound (MUB). With the MUB method, the responses are obtained by combining the seismic demands resulting from the conventional pushover analysis and UB method. Furthermore, Poursha and Samarin (2015) also extended this method to one-way asymmetric-plan tall building structures in which the effects of higher modes and torsion are significant.

In the same context, the original N2 method (Fajfar and Fischinger 1988) was extended to consider both the torsional (Fajfar et al. 2005) and the higher mode effects (Kreslin and Fajfar 2011). Fajfar and his co-workers (Kreslin and Fajfar 2012) proposed an extended

version of the original N2 method, which overcomes simultaneously the torsional and higher mode effects on buildings by adjusting the pushover results, computed with the original N2 method, through correction factors based on linear dynamic response spectrum procedures.

On another issue, adaptive lateral load has been implemented by several authors in an attempt to follow the redistribution of inertia forces related to the change effect of dynamic characteristics during the inelastic response (Gupta and Kunnath 2000; Antoniou and Pinho 2004b; Shakeri et al. 2010; Abbasnia and Tajik Davoudi 2013). Antoniou and Pinho (2004a) for the first time have developed a single-run force-based adaptive pushover analysis and then, proposed a displacement-based adaptive procedure (Antoniou and Pinho 2004b) to take into account the effects of sign reversal in the higher modes. Bento et al. (2010) applied a 3D adaptive capacity spectrum method (ACSM) along with other methods to one asymmetric-plan buildings, the well-known SPEAR building. In order to overcome the limitation of ASCM in reproducing in an accurate fashion the torsional motion of plan-asymmetric 3-D buildings, an extended ACSM was proposed by Bhatt and Bento (2014). All these methods, based on force or displacement-based adaptive procedures, provide accurate seismic responses in most of the cases but require high computational effort.

The consecutive modal pushover (CMP) procedure was proposed by Poursha et al. (2009) for estimating the seismic demands of tall buildings. In this method, the final structural responses are determined as an envelope of the results derived from a single-stage and multi-stage pushover analyses. In this method, the multi-stage pushover analysis controls the seismic responses at mid and upper storeys of tall buildings however the response of lower storeys is estimated using the single-stage pushover analysis. In (Poursha et al. 2014), an extended CMP was suggested for estimating the seismic demands of two-way asymmetric-plan tall buildings subjected to bi-directional seismic ground motions taking into account both, the effects of higher modes and torsion.

In the present work, a procedure is proposed to improve the upper-bound analysis (IUB) using a correction factor to modify the formula of the applied lateral load and the target displacement to account more adequately for the higher mode contribution. This can control only the seismic response at the upper storeys. In order to obtain an appropriate load distribution in a single-run procedure the applied load vector is calculated as the envelope of three load vectors; namely, the uniform load pattern, the first mode load pattern and the improved upper bound which will benefit from the advantages of each of the three patterns to control the seismic responses along the height of the building. This procedure (IUB) is applied to few test buildings, including medium and high-rise steel frames, and the results in terms of displacements and drifts are compared to those obtained from the nonlinear time history analysis (NTHA) as well as the MPA, the upper-bound (UB) analysis and the modified upper bound (MUB) analysis.

2 The improved upper-bound (IUB) pushover procedure

The two important features of the upper-bound pushover method are the determination of the applied load pattern and the target displacement which take into account the higher mode effect. Improvement is made by acting on both features as given below.

2.1 The applied load pattern

In the upper-bound (UB) pushover procedure (Jan et al. 2004), it is assumed that only the two first modes have an important influence on the seismic response of buildings. The effect of the other higher modes is then neglected. Thus, the applied load pattern to be used in the UB method is obtained by:

$$f_s = F_1 + F_2 = \omega_1^2 m \varphi_1 + \omega_2^2 m \varphi_2 \left(\frac{q_2}{q_1} \right)_{UB} \tag{1}$$

where F_1 and F_2 are the modal loads (Fig. 1)

$$F_1 = \omega_1^2 m \varphi_1 \tag{2}$$

$$F_2 = \omega_2^2 m \varphi_2 \left(\frac{q_2}{q_1} \right)_{UB} \tag{3}$$

in which ω_1 and ω_2 are the natural frequencies of the first and second mode respectively; φ_1 and φ_2 are the corresponding normalized mode shapes; m is the mass matrix of the structure and q_1, q_2 are the generalized coordinates of mode 1 and 2 (Jan et al. 2004). The ratio $(q_2/q_1)_{UB}$ is defined according to the following equation:

$$\left(\frac{q_2}{q_1} \right)_{UB} = \left| \frac{\Gamma_2 D_2}{\Gamma_1 D_1} \right| \tag{4}$$

where Γ_1, Γ_2 are the modal participation factors of the two modes of vibration and D_1, D_2 are the spectral displacements obtained from the elastic displacement response spectrum. It is clear that the applied load pattern is obtained in the UB procedure by a sum combination of the two first modes, and then, the effect of the second mode (negative sign) has an important influence on the shape of the load pattern (Fig. 1).

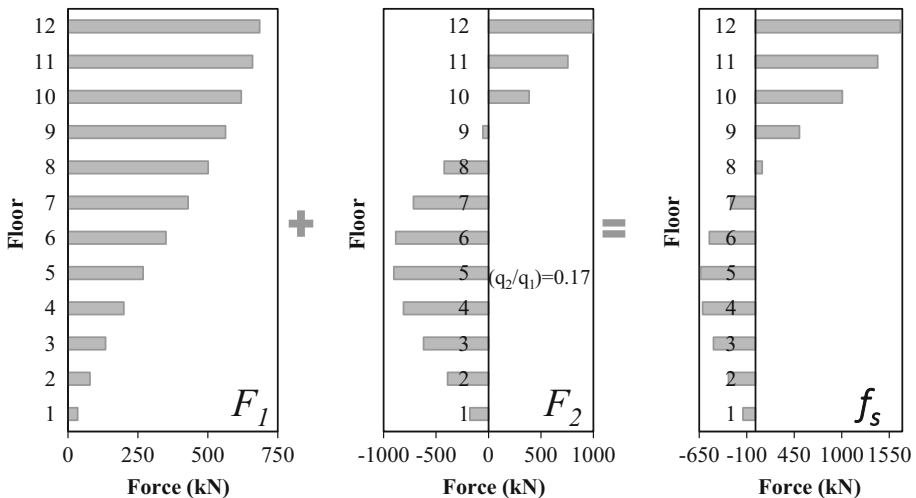


Fig. 1 UB applied lateral load pattern for a 12-storey building for level 1 set ground motions (Table 8)

Jan et al. (2004) concluded that the use of this lateral load distribution underestimates the seismic demand at lower storeys in tall buildings and overestimates at upper storeys. To overcome this shortcoming, an improved upper-bound (IUB) procedure is proposed in this paper by introducing a correction factor C_r to calibrate the contribution of the second mode to the lateral load pattern. Hence, the lateral load pattern can be expressed by Eq. (5).

$$f_s = \omega_1^2 m \phi_1 + \left(\omega_2^2 m \phi_2 \left(\frac{q_2}{q_1} \right)_{UB} \right) \cdot C_r \tag{5}$$

The correction factor C_r varies from 0 to 1. The lowest limit corresponds to the response of the conventional pushover analysis with first mode load pattern ($C_r = 0$) (i.e. the load pattern depends only on the first mode of vibration):

$$f_s = \omega_1^2 m \phi_1 \tag{6}$$

On the other hand, the upper limit for $C_r = 1$ corresponds to the response of the lateral load pattern expressed by Eq. (1), as proposed in UB procedure (Jan et al. 2004) where the effect of the second mode of vibration is fully included.

In order to determine the most fitting value of the correction factor C_r , an optimization approach is used where C_r is taken as the variable parameter in the interval [0, 1]. The storey drift along the height of the structure is the object function constrained by the NTHA drift storey profile. The 20-storey SAC building made of steel moment resisting frame is used as a generic frame. The structural characteristics and the modelling of this structure is described in Sect. 3.1. Five strong motion records are selected (Table 1) and scaled to give five different intensity levels (for Northridge-01 (Table 1) earthquake, the maximum scale factor is 3 because this earthquake has high intensity), to ensure that the structure will deform well into the inelastic range. For each case eleven pushover analyses are performed, applying the f_s load pattern (Eq. 5) corresponding to 11 correction factor varying from 0 to 1. The results (storey drift) from the pushover analyses are compared with those obtained through nonlinear time history analyses (NTHA) performed for each record individually at each intensity level. The target displacement is taken equal to the maximum roof displacement of the NTHA. The mean error—Eq. (7)—along the upper half height of the frame in which higher modes have a significant effect (Ghahari et al. 2013; Poursha and Samarin 2015) is used to measure the accuracy of the pushover analysis for a given value of C_r compared to the NTHA results.

Table 1 Earthquake ground motions details

ID	Earthquake name	Year	Station name	M_w	R_{jb} (km)	PGA (g)	Scale Factors
1	Imperial Valley	1940	El Centro array #9	6.95	6.09	0.28	(1.0, 1.5, 2.0, 3.0, 5.0)
2	Northridge-01	1994	Sylmar-Olive View Med FF	6.7	5.3	0.84	
3	Chi–Chi	1999	CHY028	7.62	3.12	0.64	
4	Loma Prieta	1989	BRAN	6.93	3.85	0.46	
5	Kobe	1995	Kakogawa	6.9	22.5	0.32	

M_w Earthquake magnitude

R_{jb} Distance to fault rupture

$$Error(\%) = 100 \times \frac{1}{n} \sum_{i=1}^n \left| \frac{\Delta_{i-push} - \Delta_{i-NTHA}}{\Delta_{i-NTHA}} \right| \tag{7}$$

In this expression, Δ_{i-push} and Δ_{i-NTHA} are the storey drift at i th storey obtained by pushover and NTHA analyses, respectively, and n is the number of storeys considered. The mean errors corresponding to pushover analysis performed using Eq. (5) with different values of C_r are depicted in Fig. 2. Generally, for all intensity levels, the lowest values of the mean errors range between $C_r = 0.3$ and $C_r = 0.6$ with less than 10% in the most cases. It can be observed that $C_r = 0.5$ is the optimal value with mean error less than 7% (Figs. 2, 3).

The same C_r value can be obtained using a different approach based on the new expression of the applied lateral load proposed by the study of Davoudi et al (2016). In this expression the applied load pattern using the first three modes is given by:

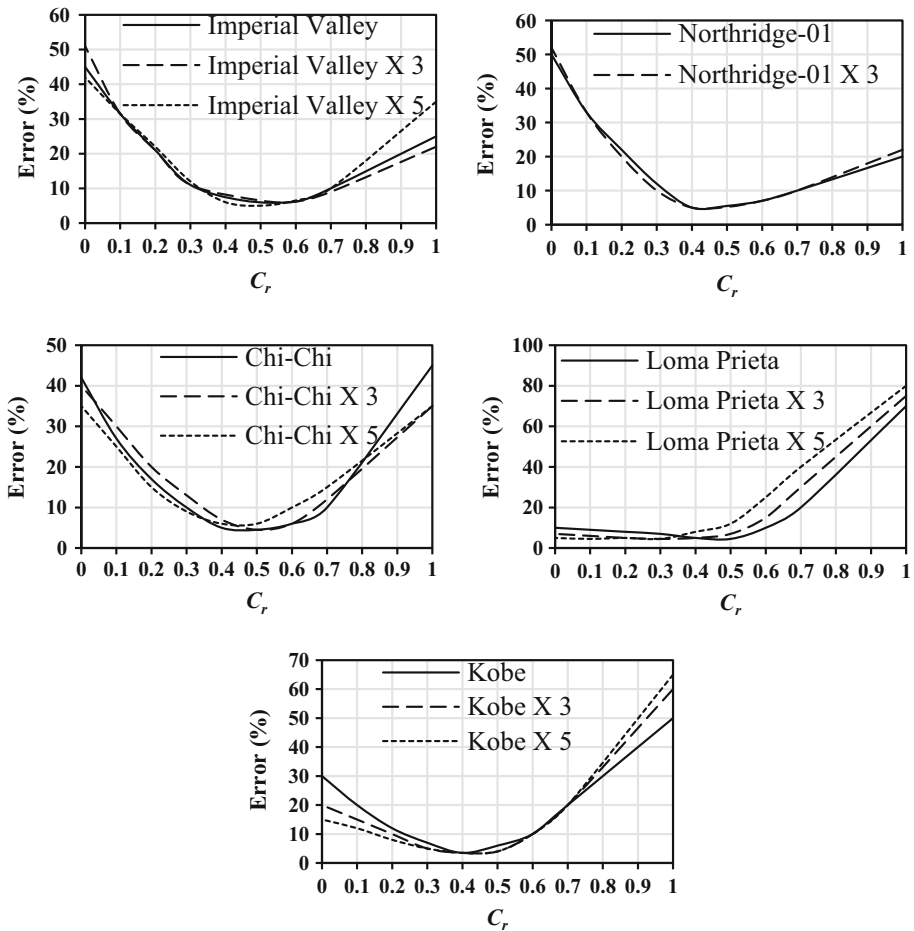
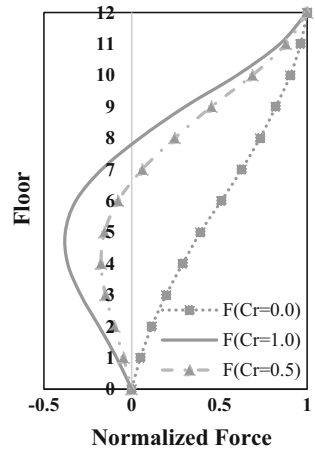


Fig. 2 Observed mean errors of storey drifts at the upper half of the SAC-20 frame using different values of C_r

Fig. 3 The corrected UB applied load pattern using three values of C_r for a 12-storey building



$$F_s = 0.48F_1 \pm 0.26F_2 \pm 0.26F_3 \tag{8}$$

Neglecting the effect of the third mode of vibration, F_s can be written as:

$$F_s = 0.48(\omega_1^2 m \phi_1 q_1) \pm 0.26(\omega_2^2 m \phi_2 q_2) \tag{9}$$

If in Eq. (9) the factor $0.48q_1$ is highlight, the following equation is obtained:

$$F_s = 0.48q_1 \left[\omega_1^2 m \phi_1 \pm \omega_2^2 m \phi_2 \left(\frac{q_2}{q_1} \right) \times \frac{0.26}{0.48} \right] \tag{10}$$

Because, in pushover analyses, the load starts from zero, the factor $0.48q_1$ has no effect on the load shape, and when considering only the plus sign Eq. (10) can be written in the form of Eq. (5), as follow:

$$F'_s = \omega_1^2 m \phi_1 + \left(\omega_2^2 m \phi_2 \left(\frac{q_2}{q_1} \right) \right) \times \frac{0.26}{0.48} \tag{11}$$

By identification of Eq. (5) and Eq. (11), the value of C_r can be obtained as:

$$C_r = \frac{0.26}{0.48} \approx 0.5 \tag{12}$$

Based on the abovementioned, the load vector f_s is determined from Eq. (13):

$$f_s = \omega_1^2 m \phi_1 + \left(\omega_2^2 m \phi_2 \left(\frac{q_2}{q_1} \right)_{UB} \right) \cdot 0.5 \tag{13}$$

In IUB procedure, instead of using the envelope of responses in multi-runs, an envelope load pattern F_s is defined using the three lateral load patterns (uniform f_{s1} , first mode f_{s2} and the improved upper bound load f_{s3} distributions). In fact, these three load patterns are combined to get a single run procedure, with an envelope lateral load pattern capable to control both seismic responses at lower and upper storeys of buildings.

The first term f_{s1} represents the uniform load pattern:

$$f_{s1} = r_U m_i \omega_1^2 \tag{14}$$

where, m_i is the mass of the i th floor. In Eq. (14) r_U is set equal to 0.8 to ensure that the uniform load distribution is dominant at lower and mid storeys of the building because the uniform load gives good estimations of responses at these levels (Poursha and Samarin 2015). It should be noted that, if r_U is equal 1.0 the uniform load controls the response and there is no need to use f_{s2} (Fig. 4b). Also, a value of r_U less than 0.8 can limit the work of the uniform load distribution (Fig. 4a). A factor of $r_U = 0.8$ allows the other load patterns to control the response at upper storeys (Fig. 4c). The first mode load pattern f_{s2} , can be obtained by

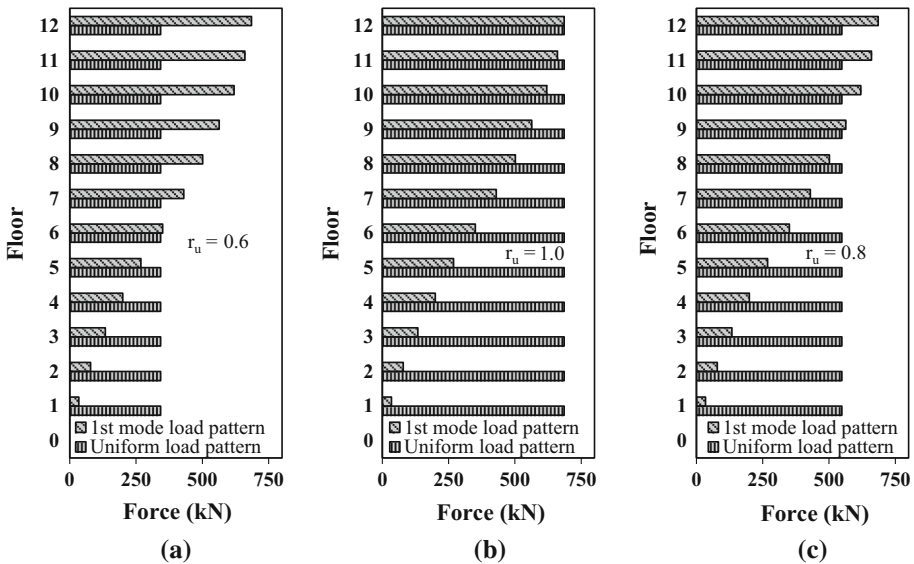


Fig. 4 The uniform f_{s1} and first mode f_{s2} lateral load patterns using different factor to reduce the magnitude of the uniform load

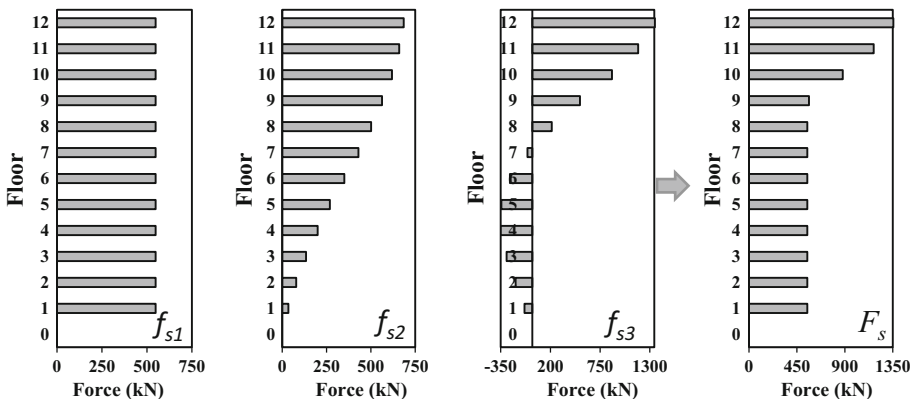


Fig. 5 The process of determining the applied lateral load pattern in the IUB for a 12-storey building

$$f_{s2} = m_i \omega_1^2 \varphi_{i1} \tag{15}$$

φ_{i1} , is the i th floor component of the normalized first mode shape. The IUB lateral load f_{s3} is given by:

$$f_{s3} = \omega_1^2 m_i \varphi_{i1} + \left(\omega_2^2 m_i \varphi_{i2} \left(\frac{q_2}{q_1} \right)_{UB} \right) \cdot 0.5 \tag{16}$$

Finally, the distribution of the applied load pattern at the i th floor F_{si} can be given by:

$$F_{si} = \max(f_{s1i}, f_{s2i}, f_{s3i}) \tag{17}$$

An example of determining the applied lateral load pattern in the IUB for a 12-storey building is graphically presented in Fig. 5.

2.2 The target displacement

The target displacement in UB pushover analysis at the roof of the structure U_r , as proposed in (Jan et al 2004), is determined using:

Table 2 Summary of UB, MUB and IUB Procedures

UB	MUB	IUB
1. Calculate the natural frequencies, ω_n , and the mode-shapes φ_n , such that the lateral component of φ_n at the roof equals unity		
2. Using the elastic response spectrum of the selected earthquake to determine the upper-bound of the contribution of the 2nd mode $(q_2/q_1)_{UB}$ as given by Eq. (4)		
3. Determine the distribution vector of the lateral loads over the height of the building using Eq. (1)		3. Calculate the distribution vector of the lateral loads over the height of the building using Eq. (13)
4. Determine the target roof displacement U_r as given by Eq. (18)	4. Determine the target roof displacement U_r .	4. Determine the target roof displacement U_r using Eq. (19)
5. Perform a pushover analysis using the lateral load calculated in step 3 until the target displacement computed in step 4 is reached (single-run analysis)	5. Perform two pushover analyses: 5.1. A pushover analysis using the load vector computed in step 3 until the target displacement defined in step 4 is reached 5.2. A pushover analysis with a uniform or triangular load pattern (multi-run analysis)	5. Perform a pushover analysis using the lateral load calculated in step 3 until the target displacement computed in step 4 is reached (single-run analysis)
6. Determine the interested seismic responses (e.g. storey drifts, element internal forces, etc.) at the step corresponding to the target displacement from the single-run in previous step	6. Determine the interested seismic responses (e.g. storey drifts, element internal forces, etc.) by enveloping the results from the two analyses computed in step 5 at the step corresponding to the target displacement	6. Determine the interested seismic responses (e.g. storey drifts, element internal forces, etc.) at the step corresponding to the target displacement from the single-run in previous step

Fig. 6 Geometric configurations of steel frames. **a** 9-storey building, **b** 12-storey building, **c** 15-storey building, **d** 20-storey building, **e** 20-SAC building

$$U_r = U_{rTLP} \left(1 + \left(\frac{q_2}{q_1} \right)_{UB} \right) \quad (18)$$

where U_{rTLP} is the target displacement at the roof of the building calculated using the capacity spectrum method (CSM) defined in ATC-40 (ATC 1996) by applying a triangular inverted load pattern. In IUB method, the same correction factor, of the one adopted for the lateral load pattern, is used to adjust the target displacement, and the expression becomes:

$$U_r = U_{rM1} \left(1 + \left(\frac{q_2}{q_1} \right)_{UB} \cdot 0.5 \right) \quad (19)$$

In the above equation, instead of adopting the triangular load pattern, the first mode load pattern is used to calculate the target displacement U_{rM1} . In fact, the procedure becomes easier this way as the first mode load distribution needs also to be defined in the subsequent steps of IUB.

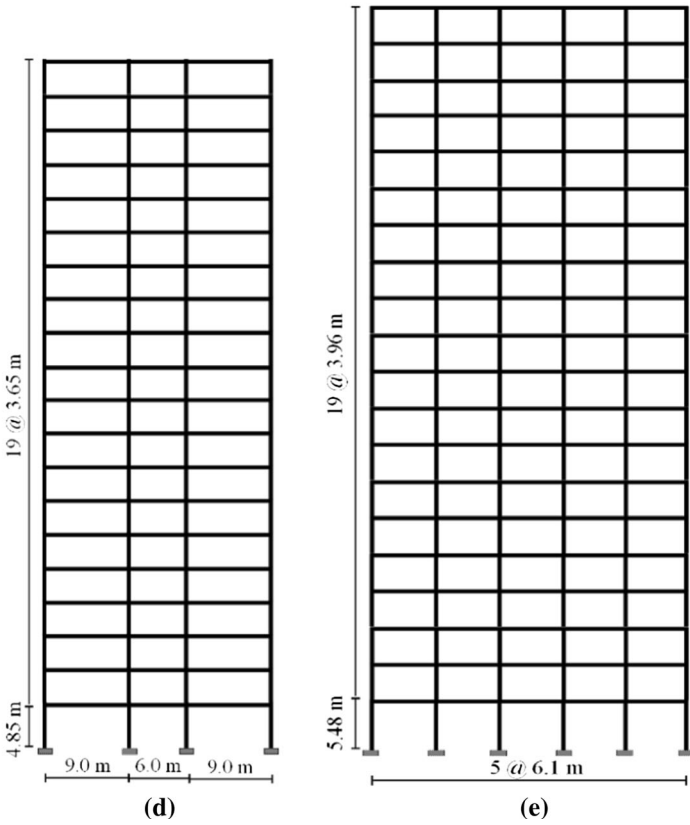
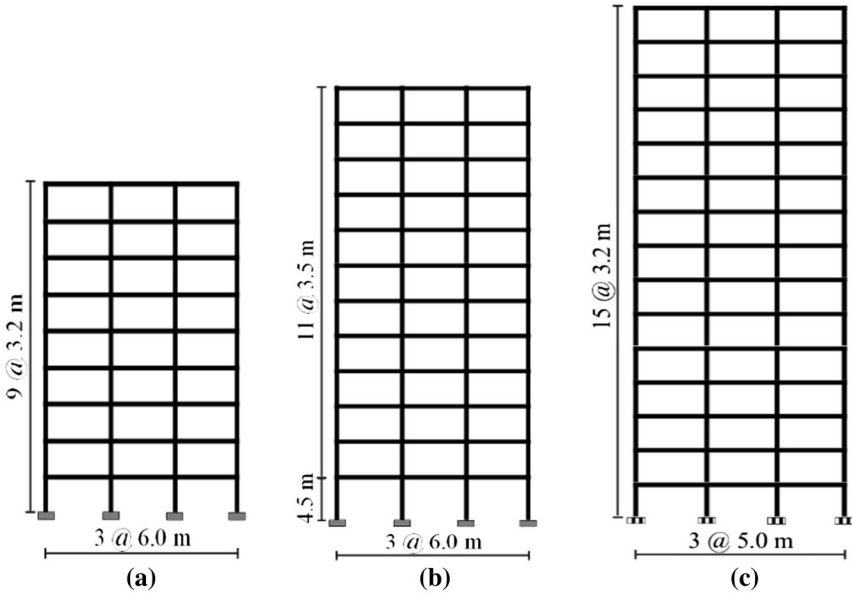
The main steps of the proposed IUB pushover procedure, are summarized in Table 2 (third column), together with those of UB and MUB procedures.

3 Numerical analyses

3.1 Structures description

To validate the proposed IUB method, five steel moment resisting frames with different geometric configurations were chosen for case studies. These are steel resisting frames having 9, 12, 15 and 20-storeys (for the latter two frames were analysed), selected from literature (Poursha and Samarin 2015; Poursha et al. 2009; Tarta and Pintea 2012; Yousuf and Bagchi 2009; FEMA 355C 2000b; Gupta and Krawinkler 1999). The 9 and 15-storey frames (Fig. 6a, c) are two special moment-resisting frames (SMRF) representing two structures designed according to the Iranian seismic code (Standard No. 2800-05 2005). These structures are located in high seismicity region and on type II (firm) soil. The two frames were three-bays, the length of the bays is 6 m in 9-storey frame and 5 m for the 15-storey frame with a uniform storey high of 3.2 m for both frames. The 12-storey moment-resisting steel frame (Fig. 6b) is designed according to Eurocode 8 (CEN 2004) and the Romanian Seismic design code (P100-1/2006 2006). The structure has three bays with 6 m length (Tarta and Pintea 2012). For this structure, the height of first storey is 4.5 and 3.5 m for others. The 20-storey frames shown in Fig. 6d is designed according to the National Building of Canada (NBCC 2005) as a ductile moment resisting frame. The structure has three bays, two exterior bays are 9 m and the interior one is 6 m in length. The height of the first storey is 4.85 m and others are of 3.65 m each (Yousuf and Bagchi 2009). The second 20-storey structure studied here is denoted SAC-20 building and designed for Phase II of SAC project (FEMA 355C 2000b; Gupta and Krawinkler 1999) according to UBC94 seismic design code (1994). This structure has been widely used in case studies (Fig. 6e).

Geometric configurations of the steel frames are shown in Fig. 6. Also, the dimensions of the cross sections, mechanical properties such as materials yield strength (F_y) and



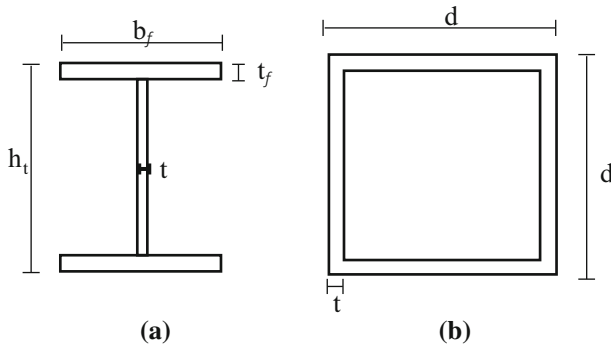


Fig. 7 Types of used sections, **a** beams, **b** columns (Poursha and Samarin 2015)

Table 3 Types and dimensions of beams and columns for the 9 and 15-storey buildings

Dimensions of beams					Dimensions of columns		
Section	h_t (cm)	t_w (cm)	b_f (cm)	t_f (cm)	Section	d (cm)	t (cm)
B1	25	0.6	17.5	1.5	C1	25	1.5
B2	30	0.8	15	1.5	C2	30	2
B3	30	0.8	20	1.5	C3	35	2.5
B4	35	0.8	22.5	2	C4	40	2.5
B5	40	1	22.5	2	C5	45	3

young's modulus (E) are presented in Fig. 7, Tables 3 and 4. The gravity loads (dead and live loads) which considered to be uniformly distributed on the beams, together with the concentrated floor masses are included in Table 5. More details about these structures can be found in references (Poursha and Samarin 2015; Poursha et al. 2009; Tarta and Pintea 2012; Yousuf and Bagchi 2009; FEMA 355C 2000b; Gupta and Krawinkler 1999).

3.2 Seismic loading

Two sets of 7 ground motion records having different intensity levels were selected to be applied to the different structures with various q_2/q_1 ratios. (The results obtained for different frames are depicted in Table 8). All the records are extracted from the PEER (2016) (Pacific Earthquake Engineering Research Centre) strong-motion database. The records in level 2 set were scaled up to a Peak Ground Acceleration (PGA) of 1 g, to ensure that all the structures will deform well into the inelastic range. More characteristics of the selected ground motion records are listed in Tables 6 and 7. The elastic pseudo-acceleration spectra with 5% damping ratio of two-level sets (herein called level 1 and level 2) are shown in Fig. 8, respectively.

3.3 Modelling issues

The elastic modal analysis, the NSPs and the nonlinear time history analysis (NTHA) were carried out using the computer program SAP2000 (Computers and Structures 2013). Elastic elements coupled with concentrated plastic hinge (nonlinear rotational spring) at

Table 4 Beams and columns of the studied buildings

Building	Story	Exterior columns	Interior columns	Beams	Mechanical properties
9-storey	1–2	C3	C5	B2	$F_y = 235$ MPa $E = 200$ GPa
	3–5	C3	C4	B2	
	6–7	C2	C3	B2	
	8–9	C1	C2	B1	
12-storey	1–2	HE800B		IPE600	$F_y = 355$ MPa $E = 210$ GPa
	3	HE600B		IPE600	
	4	HE600B		IPE600	
	5	HE600B		IPE500	
	6–9	HE500B		IPE500	
	10–12	HE400B		IPE500	
15-storey	1–4	C4	C5	B4	$F_y = 235$ MPa $E = 200$ GPa
	5–10	C3	C4	B3	
	11–12	C2	C3	B3	
	13–15	C1	C2	B1	
20-storey	1–5	W310X283	W360X314	W310X129	$F_y = 345$ MPa $E = 200$ GPa
	6–10	W310X253	W360X287	W310X129	
	11–15	W310X202	W360X262	W310X129	
	16–19	W310X179	W360X262	W310X129	
	20	W310X179	W360X262	W310X107	
SAC 20	See FEMA 355C (2000b) and Gupta and Krawinkler (1999)				

Table 5 Gravity loads and Seismic masses of the studied buildings

Frames	Floor	Dead load (kN/m)	Live load (KN/m)	Seismic mass (ton)
9-storey	Roof and floors	19.5	6.0	37.9
12-storey	Roof and floors	24.0	12.0	52.3
15-storey	Roof and floors	16.3	5.0	32.2
20-storey	Roof	17.0	11.6	47.3
	Typical floors	22.3	12.0	61.8
SAC 20	Roof	12.1	7.3	50.4
	Typical floors	17.5		53.2

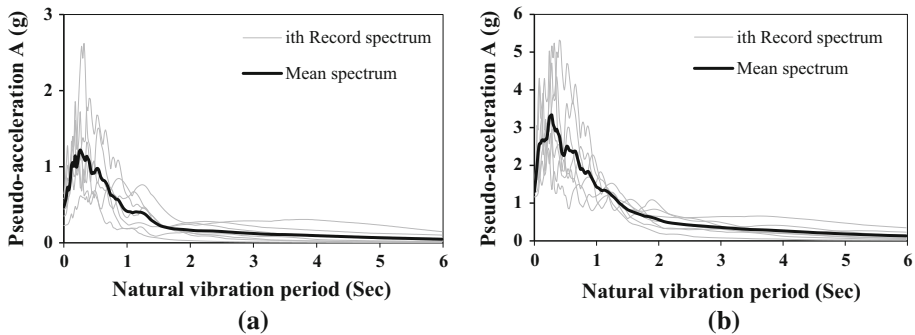
the end of the structural elements were adopted. The characteristics of the plastic hinges at the ends of beams and columns are defined according to FEMA-356 (2000a). Interaction between axial forces and bending moment is considered for the columns, while for beams only the bending moment are contemplated to control the develop of hinges. The generalized force-deformation relationship model used for modelling the hinges is shown in Fig. 9. More details about the determination of a, b and c parameters of the model in Fig. 9 can be found in FEMA-356 (2000a). The P- Δ effect is also included in this study, for both nonlinear static and dynamic analyses.

Table 6 Details of the level 1 set of records

ID	Earthquake name	Year	Station name	M_W	R_{jb} (km)	PGA (g)
1	Imperial Valley	1979	El Centro Differential Array	6.53	5.09	0.353
2	Kocaeli	1999	Yarimca	7.51	1.38	0.227
3	Loma Prieta	1989	BRAN	6.93	3.85	0.456
4	Northridge	1994	Newhall - Fire Sta	6.69	3.16	0.583
5	Parkfield	1966	Cholame - Shandon Array #5	6.19	9.58	0.444
6	Superstition Hills	1987	Superstition Mtn Camera	6.54	5.61	0.582
7	Victoria	1980	Cerro Prieto	6.33	13.8	0.645

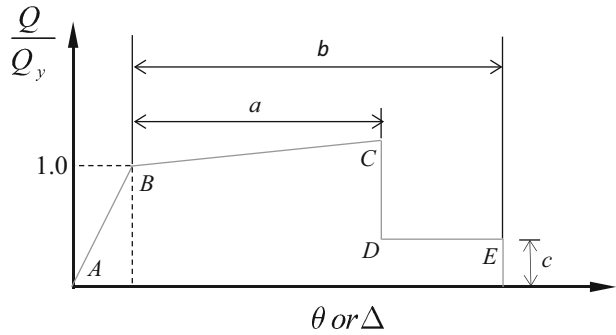
Table 7 Details of the level 2 set of records

ID	Earthquake name	Year	Station name	M_W	R_{jb} (km)	PGA (g)
1	Chi–Chi	1999	CHY028	7.62	3.12	0.636
2	Gazli	1976	Karakyr	6.80	3.92	0.702
3	Landers	1992	Lucerne	7.28	2.19	0.725
4	Loma Prieta	1989	BRAN	6.93	3.85	0.456
5	Northridge	1994	Newhall - Fire Sta	6.69	3.16	0.583
6	Tabas	1978	Tabas	7.35	1.79	0.854
7	Victoria	1980	Cerro Prieto	6.33	13.8	0.645

**Fig. 8** Mean and individual scaled pseudo-acceleration responses spectra. **a** Level 1 records, **b** level 2 scaled records

For the NTHA the Newmark step-by-step numerical integration scheme were used to perform the analysis solution. The Rayleigh damping was introduced for the direct time integration analysis, considering 5% damping ratio for the first and third modes of vibration (Chopra 2012).

Fig. 9 Generalized force-deformation relationship for plastic hinges (FEMA 356)



4 Results and discussions

The improved upper bound (IUB) procedure is validated by comparing the results of IUB with those from nonlinear time history analyses NTHA (mean response of each set of 7 records), in terms of displacement and inter-storey drift ratio at floors levels. Furthermore, to show the enhancement of IUB method compared to other existing NSPs, the responses from UB, MUB and the MPA are also added to this comparison study.

In the following section some initial results, crucial to perform the NSPs (§4.1) are first presented then the comparison of the results from NSPs and NTHA is shown and discussed (§4.1).

4.1 Preliminary results

To perform the first two steps of UB, MUB and IUB method (Table 1) it is necessary to evaluate the dynamic characteristics of the structures and the ratios q_2/q_1 —Eq. (4). The first three periods derived from the elastic modal analysis and the ratio for the two sets of records (level 1 and 2) of all the buildings are presented in Table 8.

For UB and MUB procedures, the target displacement is computed using Eq. (18). Concerning IUB procedure, Eq. (19) is proposed for the evaluation of the target displacement based on a sensitive analysis performed in a preliminary phase of this work. Some of the results obtained are presented in the following paragraph.

Table 8 Periods for the first 3 modes of vibration (T_1, T_2 and T_3) and (q_2/q_1) for the five building structures

Frame	Total height (m)	Periods (s)			(q_2/q_1) Level (1)	(q_2/q_1) Level (2)
		T_1	T_2	T_3		
9-storey	28.8	1.72	0.57	0.31	0.20	0.10
12-storey	43.0	1.65	0.57	0.33	0.23	0.17
15-storey	48.0	2.27	0.79	0.47	0.19	0.14
SAC-20	80.7	1.72	0.60	0.35	0.21	0.16
20-storey	74.2	4.73	1.56	0.90	0.11	0.17

Table 9 shows the peak roof displacement obtained from (i) NSPs previously described in Table 1; and (ii) NTHA, for the two levels of ground motion (levels 1 and 2). The differences between (i) and (ii) are presented in Table 10.

These results show clearly that the intensity level of the ground motions has an influence on the responses obtained by conventional pushover analysis with modal load pattern and NTHA; as expected, the differences tend to be higher for intense ground motions. In fact, for high values of seismic intensity levels the structures behaviour into the inelastic range and the inertial forces would certainly move away from the lateral distribution proportional to the elastic first mode of vibration (modal pattern).

The conventional pushover analysis underestimates the target displacement (negative sign) for all the buildings, with maximum of 12.7% for the 20-storey building. Furthermore, the values of the target displacement obtained using the upper-bound procedure are higher than those obtained from NTHA, which led to conservative results. Table 10 shows that the difference Exceeds 16% at level 1 in 12-storey building. Exceptionally, for the 20-storey frame (flexible structure) the errors are 3.4 and 3.1% at level 1 and level 2, respectively.

For the improved upper-bound procedure when using Eq. (19) the maximum error in the target displacement is 5.8% for the 9 storey in level 1. As a general conclusion based on

Table 9 Target displacements of buildings for the two levels records

Frame	U_{rNTHA}^a (cm)		U_{rFM1}^b (cm)		U_{rUB}^c (cm)		U_{rIUB}^d (cm)	
	Level 1	Level 2	Level 1	Level 2	Level 1	Level 2	Level 1	Level 2
9-storey	19.13	57.31	18.40	54.70	22.08	60.17	20.24	57.44
12-storey	19.10	59.57	18.05	52.01	22.20	60.85	20.13	56.43
15-storey	28.96	80.11	27.40	72.50	32.61	82.65	30.00	77.58
SAC-20	19.64	68.53	18.70	65.50	22.63	75.98	20.66	70.74
20-storey	57.02	145.11	53.10	127.80	58.94	149.53	56.02	138.66

^a Peak Roof displacement derived from the nonlinear time history analysis

^b Peak Roof displacement using CSM with first mode load pattern

^c Peak Roof displacement using upper-bound pushover analysis

^d Peak Roof displacement using improved upper-bound procedure

Table 10 Error in target displacements of buildings

Frame	Error in U_{rFM1} (%)		Error in U_{rUB} (%)		Error in U_{rIUB} (%)	
	Level 1	Level 2	Level 1	Level 2	Level 1	Level 2
9-storey	-3.82	-4.55	15.42	4.99	5.80	0.22
12-storey	-5.50	-12.69	16.24	2.15	5.37	-5.27
15-storey	-5.39	-9.50	12.59	3.17	3.60	-3.16
SAC-20	-4.79	-4.42	15.21	10.87	5.21	3.22
20-storey	-6.87	-11.93	3.37	3.04	-1.75	-4.44

these values, the improved procedure using a correction factor of 0.5 led to results bounded by those of the conventional and upper-bound pushover analyses, and gave close results to the NTHA with errors less than 5% in most cases.

It should be noted that, the determination of the target displacement U_{rM1} using a conventional pushover analysis with the first mode load pattern (1st mode) is required to determine the target displacements for both the UB and IUB procedures (Table 9). Figure 10 shows the intersection between the capacity spectrum of the 9-storey frame and the demand spectra of the two set records selected when using the first load pattern. After that, the determination of the target displacement of the UB and IUB methods are calculated using Eqs. 18 and 19, respectively. Figure 11 displays the target displacements obtained

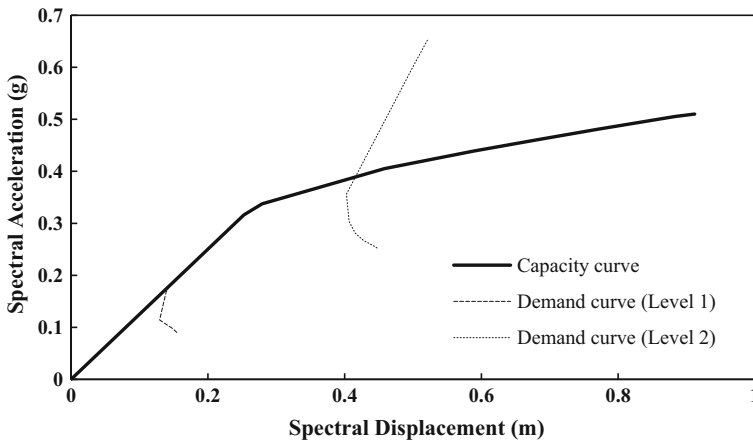


Fig. 10 The target displacement U_{rM1} determination for the two levels ground motions of the 9-storey frame

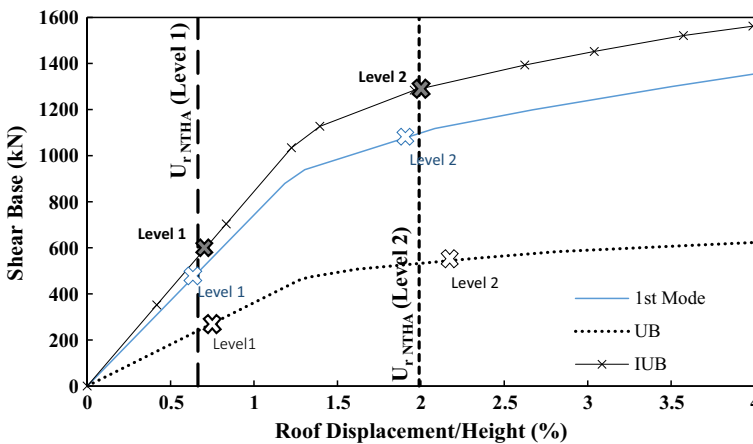


Fig. 11 Capacity curves and target displacements of the 9-storey frame obtain by different NSPs in comparison to the mean value of the maximum roof displacements from NTHA, for the two levels of ground motions

with the three procedures (1st mode, UB and IUB) and for the two intensity levels considered (Level 1 and 2).

4.2 NSPs and NTHA results

In order to evaluate the performance of the IUB, a comparison is made in terms of lateral displacement and the profiles of storey drift ratios for two levels of seismic intensities. It is worth noting that the response of the MPA procedure is obtained using SRSS combination of responses derived from the four first modes of vibration and for all the structural models.

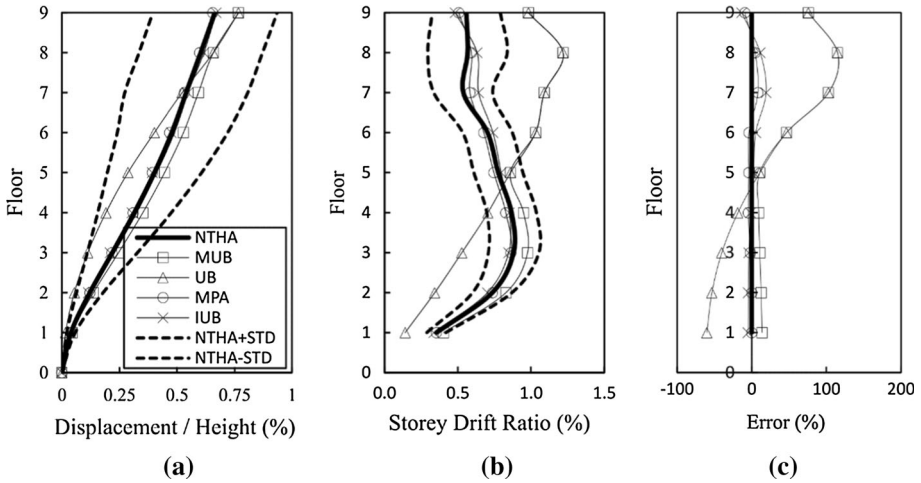


Fig. 12 Response of 9-storey building subjected to level 1 records set. **a** Displacements profile, **b** storey drift ratio profile, **c** error in storey drift

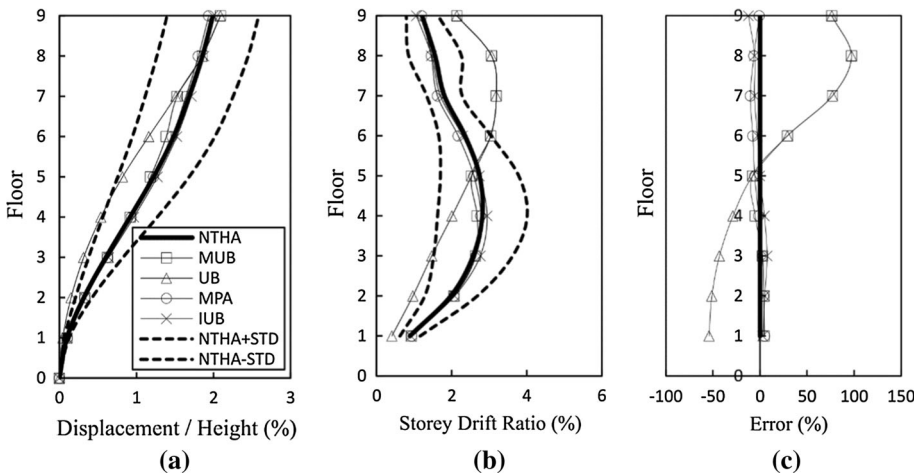


Fig. 13 Response of 9-storey building subjected to level 2 records set. **a** Displacements profile, **b** storey drift ratio profile, **c** error in storey drift

The mean responses of the NTHA plus and minus the standard deviation were denoted as $NTHA + STD$ and $NTHA - STD$, respectively.

The responses of the 9-storey frame are shown in Figs. 12 and 13, for two levels of seismic loading. The figures illustrate that the improved procedure IUB and the MPA generally lead to accurate results when compared to those of the NTHA. The UB procedure underestimates the responses at lower storeys and leads to much conservative results at the upper storeys. In the other hand, the MUB procedure benefits from the good prediction of responses at lower storeys, due to the use of the uniform load distribution which can controls the response at the lower storeys, but overestimates the results in the four upper storeys in terms of storey drift ratio and the errors (Figs. 12c, 13c) which can reach 100% at the upper storeys. The maximum errors for the MPA and IUB procedures are acceptable. For MPA the maximum errors recorded at the upper storeys are 9.1% at the 9th storey for intensity level 1 and 10.4% at the 7th storey for the level 2, while the errors in the IUB procedure reach 13.6 and 12.3% at the 9th storey for the level 1 and the level 2, respectively.

Figures 14 and 15 present the results for the 12-storey building. It shows that the UB method fails to predict the displacements and storey drift ratio at lower storeys for the two intensity levels. The MUB method provides better estimates than the UB at lower storeys for the level 1, with an error of 8.4% at the 6th storey; nevertheless, for intensity level 2 the storey drift values are underestimated up to 18%. As verified for the 9-storey building, the MPA and the IUB methods produce satisfactory estimates of displacements and storey drifts in 12-storey building. The errors obtained with MPA are smaller than those of the IUB for intensity level 1; MPA reaches a maximum of 24% at the 10th storey while, for the same floor, the difference for IUB attains 34.8%. On the other hand, for the intensity level 2, the IUB leads to more accurate results than the MPA method. The values of the storey drift at lower storeys are underestimated up to a maximum of 17.6 and 14.1% by the MPA and IUB, respectively. In the upper storeys the errors from the MPA and IUB methods reach 28.2% and 36%, respectively.

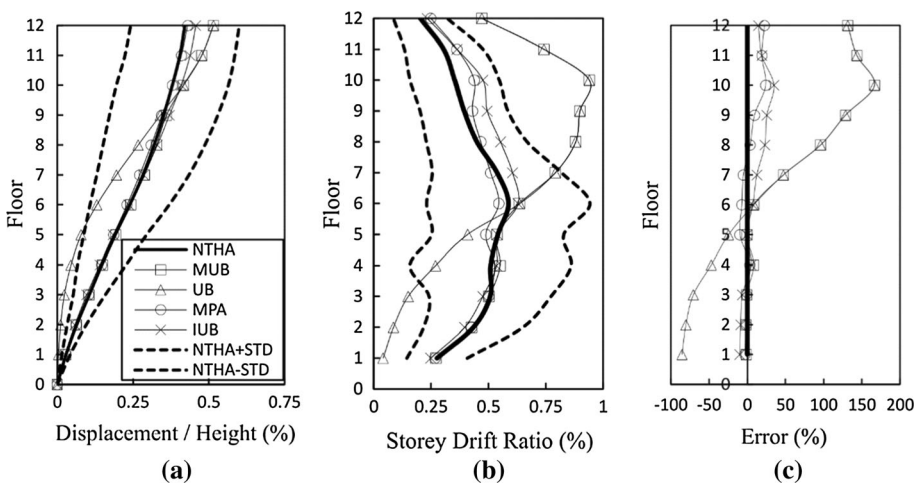


Fig. 14 Response of 12-storey building subjected to level 1 records set. **a** Displacements profile, **b** storey drift ratio profile, **c** error in storey drift

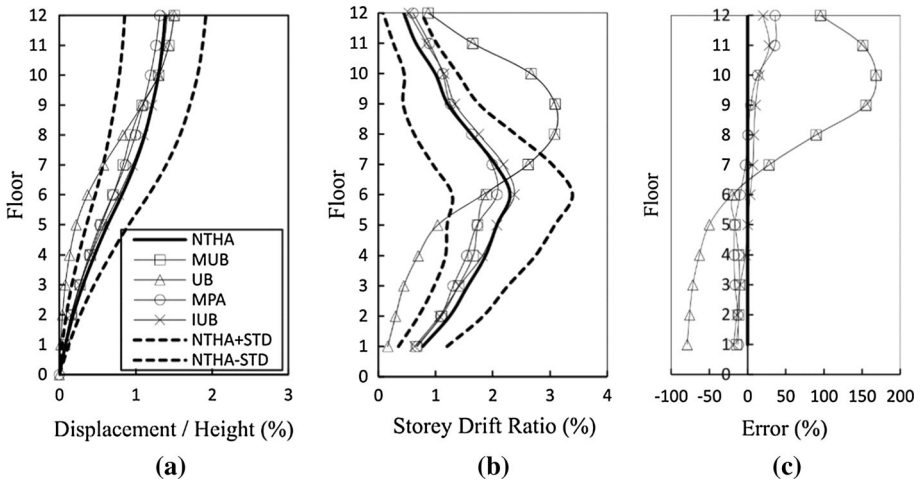


Fig. 15 Response of 12-storey building subjected to level 2 records set. **a** Displacements profile, **b** storey drift ratio profile, **c** error in storey drift

The 15-storey building, which is a more flexible structure than the 9 and 12-storey, the results obtained with UB method underestimates the response at lower storeys and overestimates at upper storeys for the two intensity levels (the error reaches 90% at the 13th storey). MPA and IUB method gives good results in level 1 and the errors in the storey drift ratio remains less than 17% for MPA and 24% for IUB. For the level 2 no procedure are able to capture exactly the response at lower storeys, but, the error is less than 25% for the MPA, MUB and IUB procedures (Figs. 16, 17). While the errors for the UB and MUB reach 200% at the upper floors, the MPA and the IUB overestimate the response at the three upper storeys with maximum error of 80% at the 14th storey.

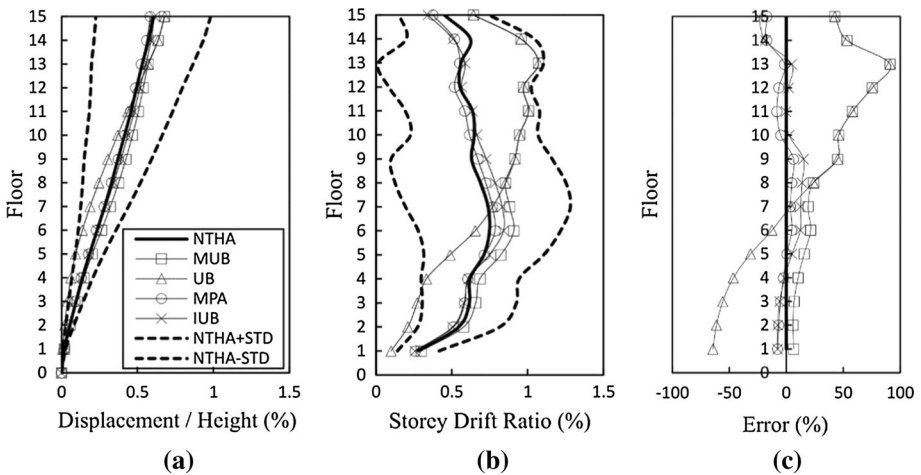


Fig. 16 Response of 15-storey building subjected to level 1 records set. **a** Displacements profile, **b** storey drift ratio profile, **c** error in storey drift

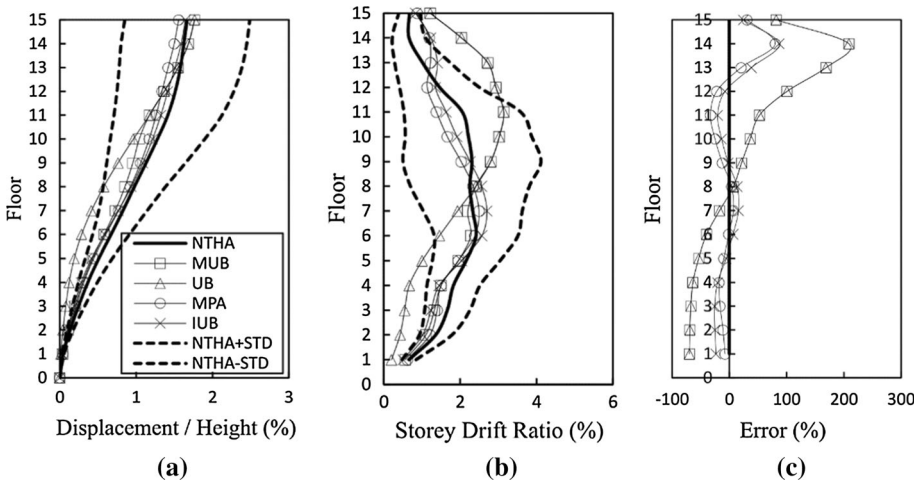


Fig. 17 Response of 15-storey building subjected to level 2 records set. **a** Displacements profile, **b** storey drift ratio profile, **c** error in storey drift

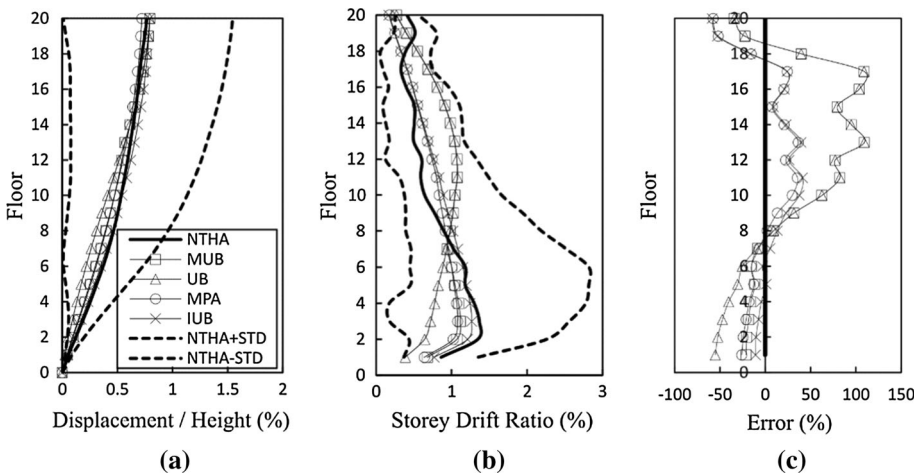


Fig. 18 Response of 20-storey building subjected to level 1 records set. **a** Displacements profile, **b** storey drift ratio profile, **c** error in storey drift

Figures 18 and 19 display the results obtained from UB and MUB of the 20-storey building which are closer to those from NTHA compared to the corresponding results of the 9, 12 and 15-storey buildings. For the level 1 records, MPA and MUB underestimate the response at lower storeys with a maximum error of 25% at the 1st storey; however, the IUB method gives good results with errors less than 10%. In mid storey, the results predicted by the MPA and the IUB methods are even closer to those resulting from NTHA in comparison to results from UB and MUB methods. In upper storeys, none of the methods is able to accurately predict the response.

For the intensity level 2, MPA and MUB are still underestimating the drift storey ratios at lower storeys, whereas, the IUB leads to conservative results with 17% maximum error

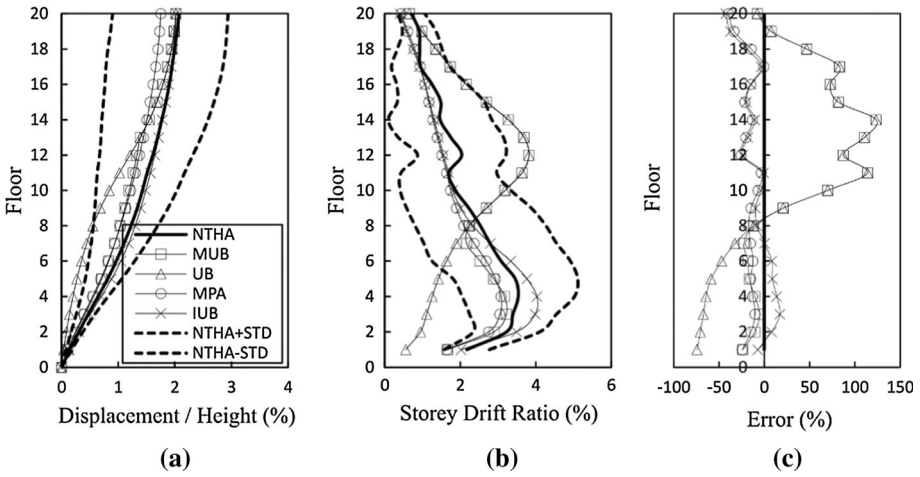


Fig. 19 Response of 20-storey building subjected to level 2 records set. **a** Displacements profile, **b** storey drift ratio profile, **c** error in storey drift

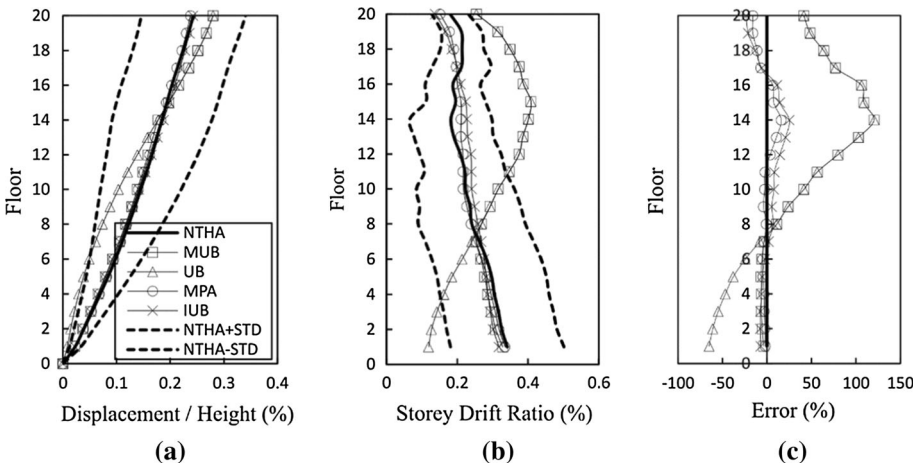


Fig. 20 Response of 20-storey SAC building subjected to level 1 records set. **a** Displacements profile, **b** storey drift ratio profile, **c** error in storey drift

at the 3rd storey. In middle and upper storeys, it is clear in Fig. 19 that the UB and MUB significantly overestimate the responses. IUB and MPA have the same results between 8th floor and the roof with a maximum error reaching 39% at the roof.

Finally, for the SAC-20 building, results in Figs. 20 and 21 confirm that MPA and IUB methods give accurate results for both intensity levels 1 and 2. These two methods give displacements and inter-storey profiles close to those resulted from NTHA. The error reaches 23% for IUB and 16% for MPA at the roof of the building for level 1, and 25% in IUB and 23% in MPA at the 16th storey for the level 2. It should be noted however, that both methods MUB and UB were not able to predict correctly the responses in this case.

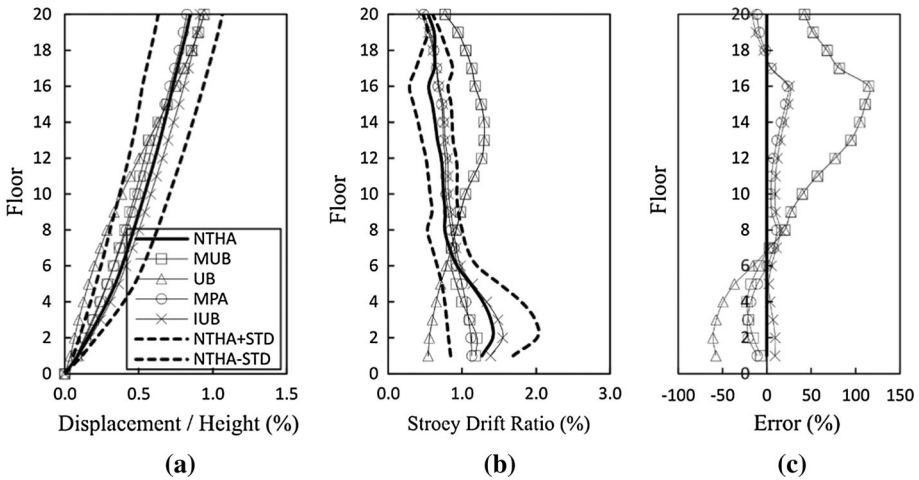


Fig. 21 Response of 20-storey SAC building subjected to level 2 records set. **a** Displacements profile, **b** storey drift ratio profile, **c** error in storey drift

5 Conclusions

This paper proposes an improved version of the upper-bound (UB) pushover method. The IUB procedure introduces a correction factor into the formula of the applied lateral load of UB method to adjust the contribution of the second mode. This factor is determined by an optimization approach which minimizes the mean error over the height of the structure with respect to the NTHA drift storey responses. For several cases at different intensity levels, it has been found that the value of the correction factor is close to 0.5. The corrected applied load pattern has been combined with the scaled uniform and first mode lateral load distributions to obtain the final (envelope) lateral load distribution. The objective is to obtain an appropriate load distribution in a single-run procedure and benefit from the advantages of each of the three patterns to control the seismic responses along the height of the building.

Moreover, the IUB procedure uses the same correction factor to evaluate the target displacement including the higher mode contribution.

In this work, the IUB is applied to a few test buildings, including medium and high-rise steel frames, and the results in terms of displacements and drifts, are compared with those of the nonlinear time history analysis (NTHA) as well as the MPA, the upper-bound (UB) and the modified upper bound (MUB) procedures. The main outcomes of this study are summarized as follows:

- The results in terms of target displacement, showed that not only the effect of the higher modes q_2/q_1 has an influence on the response, but, also the intensity level of the ground motions. The UB procedure overestimates the values of the target displacement thus leading, in most cases, to significantly conservative results in terms of displacement and inter-storey drift profiles. For high period structures ($T > 3$ s) however, like the case of the 20-storey building, the UB provides more accurate target displacement values.
- The lateral displacement and the inter-storey drifts profiles derived from IUB and MPA procedures follow closely the trend of the NTHA results for most cases considered in this study.

- While MPA, UB, MUB procedures underestimate the seismic demand at lower storeys, the IUB procedure is more accurate, but can lead to slight conservative results.

Given the type of steel frame chosen, further analyses on high-rise steel frames with significant vertical structural irregularities should be carried out to extract definite conclusions regarding the validation of this corrective factor to irregular high-rise steel frames.

Acknowledgements The financial support of the Ministry of higher education MESRS in Algeria (Grant CNEPRU J0400420140007) for conducting this study is greatly acknowledged.

References

- Abbasnia R, Tajik Davoudi A (2013) An adaptive pushover procedure based on effective modal mass combination rule. *Eng Struct* 52:654–666
- Antoniou S, Pinho R (2004a) Advantages and limitations of adaptive and non-adaptive force-based pushover procedures. *J Earthq Eng* 8:497–522
- Antoniou S, Pinho R (2004b) Development and verification of a displacement-based adaptive pushover procedure. *J Earthq Eng* 8:643–661
- ATC (1996) Seismic evaluation and retrofit of concrete buildings. Report ATC-40. Applied Technology Council, Redwood City (CA)
- Belejo A, Bento R (2016) Improved modal pushover analysis in seismic assessment of asymmetric plan buildings under the influence of one and two horizontal components of ground motions. *Soil Dyn Earthq Eng* 87:1–15
- Bento R, Bhatt C, Pinho R (2010) Adaptive capacity spectrum method for seismic assessment of 3D irregular SPEAR buildings. *Earthq Struct* 1:177–195
- Bhatt C, Bento R (2014) The extended adaptive capacity spectrum method for the seismic assessment of plan-asymmetric buildings. *Earthq Spectra* 30:683–703
- CEN (2004) ENV 1998-1 Eurocode 8: design of structures for earthquake resistance—part 1: general rules, seismic actions and rules for buildings. European Committee for Standardization, Brussels
- Chopra AK (2012) Dynamics of structures: theory and applications to earthquake engineering, 4th edn. Prentice Hall, Hong Kong
- Chopra A, Goel R (2002) A modal pushover analysis procedure for estimating seismic demands for buildings. *Earthq Eng Struct Dyn* 31:561–582
- Chopra A, Goel R (2004) A modal pushover analysis procedure to estimate seismic demands for unsymmetrical-plan buildings. *Earthq Eng Struct Dyn* 33:903–927
- Computers and Structures Inc. (CSI) (2013) SAP2000NL. Berkeley, CA, USA
- Davoudi AT, Abbasnia R, Sarvghad-Moghadam A, Maddah M-M, Khodam A (2016) An alternative modal combination rule for adaptive pushover analysis. *Struct Des Tall Spec Build* 25:325–339
- Fajfar P (1999) Capacity spectrum method based on inelastic demand spectra. *Earthq Eng Struct Dyn* 28:979–993
- Fajfar P, Fischinger M (1988) N2—a method for non-linear seismic analysis of regular buildings. In: Proceedings of the 9th World conference in earthquake engineering, Tokyo-Kyoto, Japan, pp 111–116
- Fajfar P, Marusic D, Perus I (2005) Torsional effects in the pushover-based seismic analysis of buildings. *J Earthq Eng* 9:831–854
- FEMA (2000) Prestandard and commentary for the seismic rehabilitation of buildings. FEMA 356 Federal Emergency Management Agency, Washington (DC)
- FEMA (2000) State of the art report on systems performance of steel moment frames subject to earthquake ground shaking, FEMA 355C, SAC Joint Venture and FEMA, Washington (DC)
- Freeman S (1998) The capacity spectrum method as a tool for seismic design. In: Proceedings of the 11th European conference on earthquake engineering, Paris, France
- Ghahari SF, Moradnejad HR, Rouhanimanesh MS, Sarvghad-Moghadam A (2013) Studying higher mode effects on the performance of nonlinear static analysis methods considering Near-Fault effects. *KSCE J Civ Eng* 17(2):426–437
- Gupta A, Krawinkler H (1999) Seismic demands for performance evaluation of steel moment resisting frame structures. John A, Blume Earthquake Engineering Research Center, Rep. No. 132. Department of Civil Engineering, Stanford University

- Gupta B, Kunnath SK (2000) Adaptive spectra-based pushover procedure for seismic evaluation of structures. *Earthq Spectra* 16:367–391
- Jan TS, Liu MW, Kao YC (2004) An upper-bound pushover analysis procedure for estimating the seismic demands of high-rise buildings. *Eng Struct* 26:117–128
- Kreslin M, Fajfar P (2011) The extended N2 method taking into account higher mode effects in elevation. *Earthq Eng Struct Dyn* 40(14):1571–1589
- Kreslin M, Fajfar P (2012) The extended N2 method considering higher mode effects in both plan and elevation. *Bull Earthq Eng* 10:695–715
- NBCC (2005) National building code of Canada. Canadian Commission on Building and Fire Codes, National Research Council of Canada, Ottawa, Canada
- P100-1/2006 (2006) Seismic design code. Part 1: earthquake resistant design of buildings. *Buletinul Construcțiilor*, No. 12–13. INCERC, Bucharest, Romanian
- Paraskeva TS, Kappos AJ (2010) Further development of a multimodal pushover analysis procedure for seismic assessment of bridges. *Earthq Eng Struct Dyn* 39:211–222
- Poursha M, Samarin ET (2015) The modified and extended upper-bound (UB) pushover method for the multi-mode pushover analysis of unsymmetric-plan tall buildings. *Soil Dyn Earthq Eng* 71:114–127
- Poursha M, Khoshnoudian F, Moghadam AS (2009) A consecutive modal pushover procedure for estimating the seismic demands of tall buildings. *Eng Struct* 31:591–599
- Poursha M, Khoshnoudian F, Moghadam AS (2014) The extended consecutive modal pushover procedure for estimating the seismic demands of two-way unsymmetric-plan tall building structures under influence of two horizontal components of ground motions. *Soil Dyn Earthq Eng* 63:162–173
- Reyes JC, Chopra AK (2011) Three-dimensional modal pushover analysis of buildings subjected to two components of ground motion, including its evaluation for tall buildings. *Earthq Eng Struct Dyn* 40:789–806
- Shakeri K, Shayanfar MA, Kabeyasawa T (2010) A story shear-based adaptive pushover procedure for estimating seismic demands of buildings. *Eng Struct* 32:174–183
- Standard No. 2800-05 (2005) Iranian code of practice for seismic resistant design of buildings, 3rd edn. Building and Housing Research Centre, Iran
- Tarta G, Pinteá A (2012) Seismic evaluation of multi-storey moment-resisting steel frames with stiffness irregularities using standard and advanced pushover methods. *Procedia Eng* 40:445–450
- UBC (1994) Uniform building code. International Conference of Building Officials, Whittier, CA
- Yousuf M, Bagchi A (2009) Seismic performance of a 20-story steel-frame building in Canada. *Struct Des Tall Spec Build* 19:901–921